Fracture 1977, Volume 4, ICF4, Waterloo, Canada, June 19 - 24, 1977

PLASTIC FLOW AROUND A CRACK UNDER FRICTION AND COMBINED STRESS

Frank A. McClintock*

INTRODUCTION

A boundary integral relaxation method was used to calculate the plasticity at the tip of a small horizontal crack buried in a rail head. The Hertz equations were used as boundary conditions, along with axial residual stress. A wheel passage gives initial sliding, followed by locking, squeezing the plastic zone, reversed sliding, locking, and finally unloading.

Computing four cycles of this rail stress history cost $51. At steady state (only three cycles), the plastic zone extended in the shear direction almost exactly as far as predicted from linear elastic fracture mechanics, in spite of the compression being 8 times the net shear tending to produce Mode II. The crack always remained closed. Reversed shearing on cross-slip planes was no more than 10% of that on the segment directly in front of the crack.

Some speculations are given about a fracture criterion in terms of the displacements and the compressive stresses.

THE PROBLEM

About 800 trains per year are derailed in the United States due to broken rails. The damage is over $60,000,000.00 [1]. This occurs in spite of continuous inspection by a fleet of 15 rail cars, which leads to the replacement of 200,000 defective rails per year [2]. Thus, one might say that the inspection system is 99.6% perfect. In turn, these 200,000 defective rails are only 0.2% of the rails in service, suggesting that the rails themselves are of generally good quality. Their replacement rate is very low, so that existing rails will be used for perhaps 50 years. The fundamental question giving rise to the detailed study reported here is whether reasonable improvements in inspection procedures, taking account of service loads and roadbed compliance, could reduce the loss due to derailments without too great an additional cost.

This paper is concerned with the specific problem of estimating whether or when the relatively benign shell fractures that run parallel to the rail surface will turn and become transverse breaks. The tendency of the crack to run straight or to suddenly turn a corner is presumably controlled by the macroscopic stresses due to loading, by the residual stresses in the head due to contact loads, and by the anisotropy of the fracture strength in the material itself. Other workers are making three-dimensional finite element studies of the macroscopic stress distribution. Here we shall assume a simple stress field, such as might be found from such a study, and consider some aspects of the plasticity of crack growth within that field.

* Department of Mechanical Engineering, Massachusetts Institute of Technology, Cambridge, Massachusetts, USA.

The results of this study should also be of interest in contact fatigue and also in wear, which in many cases appears to be due to progressive deformation and fracture under repeated contacts of the micro-asperities. Furthermore the numerical methods may be of interest in other cases where history or high nominal stress distorts the usual linear Irwin-Williams or non-linear Hutchinson, and Rice and Rosengren, (HRR) stress and strain fields (see e.g. [3]-[9]).

The contact area between a rail and a wheel is typically of the order of 10 mm diameter, with the point of maximum equivalent stress below the surface by 1/4 the contact diameter. Overloads cause larger contact diameter and plastic flow, which will shake down at loads up to 70% above that for initial yielding (Johnson [10]). The compressive residual stress leaves tensile stress at greater depths. There are also stresses due to bending and shear of the rail. For definiteness, neglect these and consider only the residual stress at the shakedown limit, superimposed on a repeated rolling load small enough for small scale yielding around a horizontal crack buried at the point of maximum shakedown stress. Choose the current cracking load so that the extent of the plastic zone due to the shear stress, R_{II}, taking friction into account, will not exceed some given fraction of the crack half-length a. Furthermore, consider the contact to be plane strain and the crack to be short enough so that the stress is uniform over the crack. This assumption appears reasonable for the relatively long time that any crack is short.

The elastic stress field is obtained from the known solution of Hertz. In the coordinates of Figure 1 with load per unit thickness P, half-width of contact b, and $z = (x+iy)/b$, from Radzimovsky [11] (or by Johnson [10], correcting signs and conjugates):

$$\frac{\sigma_{xx} + \sigma_{yy}}{2} = \frac{2P}{\pi b}\,\mathrm{Im}\left(\frac{1}{z/b + \sqrt{(z/b)^2-1}}\right),$$

$$\frac{\sigma_{xx} - \sigma_{yy}}{2} - i\sigma_{xy} = -\frac{2P}{\pi b}\,\frac{y/b}{z/b + \sqrt{(z/b)^2-1}}\,\frac{1}{\sqrt{(z/b)^2-1}}\,. \tag{1}$$

Johnson [10] gives the residual stress due to the maximum shakedown load per unit contact length P_m and the depth y at which it occurs in terms of the contact half-width at maximum load b_m and the tensile yield strength σ_Y in terms of the contact pressure $(2P_m/\pi b_m)$ as,

$$\sigma_{xxr} = -0.134\ (2P_m/\pi b_m)\ ,$$

$$y/b_m = 0.5\ , \tag{2}$$

$$\sigma_Y/\sqrt{3} = 0.25\ (2P_m/\pi b_m)\ .$$

The contact half-width b is in turn related to the wheel diameter D and the modulus of elasticity E by the usual equation,

$$b = \sqrt{2\ PD\ (1 - \nu^2)/\pi E}\ . \tag{3}$$

Since the crack turns out to be subjected mostly to shear, the extent of the plastic zone ahead of a crack under shear in such a stress field can be estimated from the Dugdale [12] - Barenblatt [13] yield zone. Under pure shear, with a shear yield strength of $\sigma_Y/\sqrt{3}$, with the crack faces subject to a coefficient of kinetic friction f_k, and with a normal pressure $-\sigma_{yy}$, the plastic zone extends along the crack line by

$$R/a = \sec\left(\pi(|\sigma_{xy}| - f_k|\sigma_{yy}|)\sqrt{3}\sigma_Y/2\right) - 1\ . \tag{4}$$

The reduced shear strength due to differences in normal stress components may be estimated, neglecting through-thickness stress deviators, by

$$\sigma_{Yred}/\sqrt{3} = \sqrt{\sigma_Y^2/3 - (\sigma_{xx} - \sigma_{yy})^2/4}\ . \tag{5}$$

A small computer program was developed to evaluate the stress fields and the extent of the plastic zone, assuming various fractions of the shakedown load. The resulting history of shear and normal stress applied to the region of the crack are shown in Figure 2. The history is surprisingly involved. At first, the shear stress greatly exceeds the normal stress, so sliding occurs on the crack faces. The difference between the applied shear stress σ_{xy} and the surface shear stress σ_{xysfc}, here called the net tip shear σ_{xytip}, is available to cause stress intensities at the tip of the crack. If this is started to decrease immediately after reaching a maximum, there would be a backward sliding on the crack surface. Since this would require a reversal of the surface shear stress σ_{xysfc}, locking occurs instead. This occurs even though the applied shear stress is still increasing. The crack faces remain locked as the contact point rolls over the crack. They finally break loose when the backward stress due to the stress intensity plus the applied shear stress is enough to break the surfaces loose. Reversed sliding now occurs until the reversed stress intensity due to σ_{xytip} reaches the same value which it had in the forward direction. Again, the surface is locked. This time the decreasing normal stress soon leads to reversed (now forward) sliding, and both shear and normal components of stress decrease to zero as the point of contact passes away.

I had expected that the resulting crack tip stress and strain fields could be calculated from the displacement of an elastic linear or nonlinear (HRR) strain field, coupled with a slip line field analysis for the region very close to the crack tip. From Figure 2, however, the mean normal stress is 6 to 8 times larger than the net tip shear stress. This normal stress, increasing as the contact point approaches the crack, was expected to "set in" the forward displacement. Successive forward displacements should lead to, and be inhibited by, reversed residual shear stress components. It is interesting to note that these displacements would be opposite in direction to the deformations associated with exceeding the shakedown load, where observations of Crook [14] on uncracked material show a backward sliding of a layer near the surface when the point of rolling contact is moving forward relative to the substrate. A relatively complete and exact solution seems necessary to understand this in terms of plasticity, the

Bauschinger effect, and possible strain aging. In any event, the large normal stress components mean that a small scale yielding analysis may well not be appropriate. Furthermore, the complex interaction between residual stress, any possible Bauschinger effect, mean normal stress, and current stress increments, along with fluctuating loads and the macroscopic stresses due to bending of the rail, mean that a more detailed analysis is called for. An approximate numerical method is described in the next section. As an example, the stress history of Figure 2 is taken as boundary conditions.

NUMERICAL STUDIES

The Segmented Boundary Integral Method

The computer program used for this study is based on a boundary integral method that gives repeated plane elastic solutions for incremental, history-dependent boundary conditions. It allows the modelling of problems involving crack opening and closing, stick-slip friction, and any plasticity that can be simulated by shear displacement across discrete planes at a critical resolved shear stress. The body must be elastically homogeneous. It may be either infinite in extent or bounded by a multiply-connected polygonal boundary consisting of m (for margin) straight segments.

The boundary conditions are modelled by regarding the body as being contained in an infinite elastic solid and inserting displacement discontinuities between the body and its surroundings, as shown in Figure 3. For brevity, these displacement discontinuities are called "darts". The term comes from sewing, where it denotes the removal of a strip of material and re-joining the edges, as for example, to draw in a woman's dress at her waist. For cracks and slip surfaces the boundary tractions on opposite faces are equal and opposite, and the displacements are taken to be relative displacements between the faces, with crack opening as positive. The use of darts (relative displacements) rather than loads as kernels of the integral equation is especially convenient for modelling cracks and slip surfaces within a body. To improve the accuracy, not only average tractions and displacements, but also their gradients may be specified. Correspondingly, linearly varying ("gradient") darts are used to produce the desired boundary conditions.

Darts would give infinite forces on segments, if they ran from one end of a segment to the other. This follows from the fact that, as may be seen in Figure 3, they have edge dislocations at their ends. (Normal darts have a pair of climb dislocations; shear darts have a pair of glide dislocations). The resulting 1/r stress singularities would integrate to logarithmically infinite forces of opposite sign on the two segments adjacent to any dislocation. To avoid these infinities the net dislocation of a node between segments was split and half was moved towards the other end of each segment by a fraction F of the segment length. At crack tips the entire dislocation was moved back.

Known analytic solutions for dislocations are used to give average traction vectors t and displacement vectors u^μ on each affected segment μ, due to darts D^m on that or other dislocated segments m:

$$t^\mu = T^{\mu m} D^m \ , \qquad (6)$$

$$u^\mu = U^{\mu m} D^m \ ,$$

where summation over all normal and shear, displacement and gradient components and over all segments μ is understood.

The boundary conditions are specified as general linear relations between any or all of the traction and displacement vectors. The relations are given in terms of "parameters" p^k $(k = 1,\mu_{max})$ and "coefficients" $p^{k\mu}$ by

$$p^k = p^{k\mu}_{,u} u^\mu + p^{k\mu}_{,t} t^\mu \ . \qquad (7)$$

For instance, static friction is assumed on a segment, if the prior shear stress was within the limits for incipient sliding. Then the boundary conditions on that segment are

$$u^\mu_n = 0 \ , \qquad u^\mu_s = (u_s)_{previous} \ . \qquad (8)$$

The equation $k = \mu$ in (8) is reduced to this form by taking

$$p^\mu_1 = 0 \ , \ p^{\mu\mu}_{1,t} = 0 \ , \ p^{\mu\mu}_{1,\mu} = 1 \ ;$$

$$p^\mu_2 = (u^\mu_s)_{previous} \ , \ p^{\mu\mu}_{2,t} = 0 \ , \ p^{\mu\mu}_{2,\mu} = 1 \ ; \qquad (9)$$

$$p^{k\mu}_{,\mu} = 0 \ , \text{ for } k \neq \mu \ .$$

Other friction and slip conditions are handled similarly. The decisions for crack opening or closing, for stick-slip friction, and for plastic sliding or locking are all made on the basis of the previous state, so small steps must be taken to avoid serious over-shoot.

When equations (6) for the tractions and displacements in terms of the darts are substituted into the boundary conditions (7), the loading parameters P^k are linearly related to the darts D^m:

$$p^k = (p^{k\mu}_{,t} T^{\mu m} + p^{k\mu}_{,u} U^{\mu m}) D^m \ . \qquad (10)$$

Equation (10) is solved for the darts D^m. With the darts known, stress and displacement are calculated at any points desired by the user.

The program is written in FORTRAN IV, Level G, using complex numbers. It has been run on the IBM 370-168 computer in the MIT Information Processing Center in less than 5 seconds for a 25 segment problem and a single set of boundary conditions. The core requirement is roughly $257 + .2\,(\text{segment capacity})^2$ kbytes. The program has been used for elastic calculations of fatigue crack growth under general in-plane loading by Pustejovsky [15], where it was checked against known analytical and finite element solutions. A similar elastic test will be reported below in connection with the segments finally chosen.

Verification of the Boundary Integral Method for Plasticity Around Cracks

To verify the program for plasticity, it was used with the problem shown in Figure 4, consisting of a fully plastic ligament of unit half-length between two co-linear cracks each of total length 44.1. This saved modelling the external boundaries of an externally grooved specimen. Increasing the stress applied at infinity takes the ligament to its limit load and then applies a controlled extension.

The grid of Figure 4 was chosen to allow the development of a fully plastic flow field using a small number of segments. The lower half of the specimen moves down with a unit displacement, carrying the central tongue with it. Blocks adjacent to the central tongue move inwards, while the outer ones move diagonally upward and inward to replace the material flowing through the shear zones leading down to the crack tip. Thus the material flowing into the ligament comes from an extra crack *tip* opening displacement which is 1.5 times the crack *flank* opening displacement.

As shown here, the flow field is unique. If there were a slip line across the ligament itself, the field would not be unique due to the possibility of unequal flow from either side. The numerical method would still select the deformation field shown here, which is the first that became kinematically admissible. A small amount of strain hardening would give a unique flow field, as worked out by Neimark [16].

The mean normal stress across the ligament required to produce the slip in the various shear zones is $(10/3)\sigma_Y$, versus the value of $(1+\pi/2)(2/\sqrt{3})\sigma_Y = 2.9685\ \sigma_Y$ of the exact solution for an isotropic material.

The computed displacement fields were taken to be the differences between displacements of four and eight times those at the limit load. The downward displacement increment of the material below the ligament relative to that above was normalized to unity. The analytical and *computed* displacement increments across the various slip lines and the crack face are compared in Figure 4 for the left hand side, which had the greater errors. The results are within 0.5% for all cases. The average traction across the ligament is within 2% of the expected value. The equivalent stress at the centers of the blocks is by no means as well calculated, differing from the yield strength by a factor of 1.5 either way. From other work with the computer program, this error is more likely to be due to the block sliding model adopted here than to any defect in the program itself. We therefore conclude that the computer program used here is self-consistent and gives good results within the limitations of the particular field of segments that is being considered.

The part of the program dealing with changes in frictional and stick-slip boundary conditions was checked by a complete set of some 25 combinations of initial conditions and changes, for example from an open crack to one sticking or sliding in either direction.

Choice of Grid for the Buried Crack

The grid was chosen to put slip segments where they were most needed. Preliminary runs showed that slip on radial planes out to unit radius occurred only directly in line with the crack. The desire to minimize computer costs then led to the field of segments shown in Figure 5. The missing slip plane at the top of the hexagon was left out not only to minimize the number of

segments, but also because a preliminary run with a plastic zone just above the central plane, including that segment and radial ones out beyond it, had indicated no plastic strain would occur there. The fraction F by which dislocations were moved back from crack tips was taken to be 0.001. The crack and slip segments were extended to overlap by that amount so that the dislocation sites for adjacent segments would coincide exactly.

Verification of the Program for Elasticity Around the Crack

As a further check on the program, the first step of the loading for this crack was compared with independent calculations of stress and displacement from the usual Irwin-Williams elastic singularities. Additive constant stress terms can be chosen to match either the conditions on the crack or at infinity; the conditions along the crack were matched. In order to fix rigid-body motion, the displacements were fitted to the computer results at the first point in front of the crack and the rotation was fitted to the vertical displacement of the second point.

The results for the stress were all within 6% of the maximum stress component at any point. The maximum error in mean traction occurred directly in front of the crack, where it was higher than the local stress by almost exactly $\sqrt{2}$ as expected from the $1/\sqrt{r}$ singularity. The displacements were accurate to 2% on the inner ring but the error increased to 14% at sites with radius 0.375 ($\sqrt{r/a} = 0.22$), very likely because of higher order displacement terms.

Choice of Boundary Conditions

The crack was assumed to occur at the depth giving the maximum allowable load at shakedown, and the shakedown residual stress was assumed, both according to (2). The load was then decreased to correspond to small-scale yielding, taking the expected plastic zone size calculated from (4) and (5) to be just unity for a crack half-length of a = 7.875. This particular number came from taking six segments for the total crack length 2a and doubling adjacent segment lengths, progressing outward from the crack tip of interest, where the first segment was of length 0.25. This load resulted in the following maximum values for stress components regarded as being applied at infinity:

$$\sigma_{xxr} = -0.310\ \sigma_Y\ ,$$

$$\sigma_{yymax} = -1.480\ \sigma_Y\ , \qquad (11)$$

$$\sigma_{xymax} = 0.432\ \sigma_Y\ .$$

Cost and Potential for Development

The stress cycle shown in Figure 2 was divided into 27 steps of varying size to reveal details with a small total number of steps. The program was run for four complete cycles at a total computer cost of $51. The cost could be reduced in a number of ways. Running consecutively at optimum rates would drop the cost to $34. Conditions at all segments and 11 other

points were printed out at each step, giving a printing cost of 27% of the total. Two thirds of the cost is solution time, which varies as the cube of the number of segments. The full matrix, involving 17 segments and 4 degrees of freedom per segment was solved at each stage, even though the normal displacements were known to be zero for all the plastic segments, so the matrix could be correspondingly reduced in size. (Similarly for segments that are known to be in the locked, rather than sliding, mode). Instead of translational and gradient darts, triangular darts could be introduced at each node, halving the number of degrees of freedom for the plastic elements once again, and eliminating the question of displacing dislocation sites some arbitrary distance from the node to avoid infinite forces on segments. These savings would probably be used to get more details in the plastic zone, especially at higher levels of applied stress. Some studies of load history effects could be made. Thus the method has good promise as a research tool, and to test empirical equations for the growth of cracks in rails. Even with these savings, the program is not likely to be of use for routine predictions of life in individual rails until further reductions in computer cost are available, or more understanding has been found of just which are the critical events that must be calculated.

Results and Discussion

A number of specific observations were made from looking at the computed data.

1) A steady state was nearly attained after only three cycles, since the results of the fourth differed by at most 0.2% of the maximum stress or displacement. This is half the worst round-off error, as noted by asymmetry of the fully plastic problem.

2) The crack stayed closed throughout the process. Perhaps as a result of this continued closure, the out-of-plane sliding was no more than 10% of the sliding in the plane of the crack, and the shear displacement of the crack at its tip was very nearly identical to that of the first segment beyond the crack.

3) The displacements across slip lines radiating from the crack tip were calculated from the mean displacement and displacement gradient along each radial segment, and are shown in Figure 6 for the last cycle. Consider first the results for planes at 0° and 180° from the crack, here with normalized displacements scaled down by a factor of 10. The short reversals on the curves as plateaus are approached are due to the fact that if reversed sliding was found to occur after the tractions for forward sliding had been assumed, no correction was made. Instead, the displacements were assumed locked at their *previous* values and for the *next* iteration. The short reversals before a plateau of constant displacement should therefore be ignored. Finer step sizes or an iteration procedure would reduce or eliminate them.

4) Shear on cross slip planes was out of phase, and unequal amounts of slip occurred on planes across the crack tip from each other.

5) There is a very slight forward motion of the upper half of the crack, in the direction of the rolling contact, but it was little more than the error in the elastic results.

6) The plastic zone extended primarily ahead of the crack, about as expected from the preliminary run. The extent of the plastic zone can be estimated quantitatively by extrapolating the slope of the displacements for the last segment from the mean value for that segment. This extrapolation indicated the plastic zone of forward sliding extended to 1.066 and that for reversed sliding to 1.064, surprisingly close to the value of 1 expected from the Dugdale-Barenblatt results, taking friction and normal stress into account according to (4) and (5). The stresses calculated at the point of the missing segment directly above the plastic zone indicated that shear would not be expected there except just before reversed sliding on the crack plane. There was a large difference of normal stress components, however, and check calculations should be made, allowing for the possibility of normal components of plastic strain at that point. The yield on radial planes above and below the crack was estimated by extrapolation to extend out no farther than r = 0.343. This justifies the extent of the grid chosen for possible slip, shown in Figure 5.

CRACK GROWTH CRITERION

With the displacement components at the crack tip known, the next question is to estimate the corresponding advance of the crack tip.

Shear from the Crack Tip on One Radial Plane

Slip on one radial plane from the crack tip can be thought of as being produced by a dislocation leaving the tip. The predominant mode of deformation for this loading is glide along the plane in front of the crack, shown in Figure 7a. (For a continuous flow field, one would consider the relative displacement across some finite angle $\delta\theta$.) Assume that the crack slides enough to accommodate the displacement introduced at the crack tip and that there is no rewelding. New surface will be introduced, as shown by the dashed line. The crack advance relative to the average displacement between the faces is just half the relative displacement across the glide plane. Assume there is enough compression to suppress any fracture by hole growth or cleavage in the tensile region below the tip of the crack, at A. Then the growth is purely in the glide direction. To describe any re-welding, define the "efficiency" of crack growth as the ratio of growth to half the component of the glide displacement (Burger's vector) on the crack plane:

$$\eta = da/(d|u_s|/2) \ . \qquad (12)$$

With no re-welding, the crack growth efficiency would be $\eta = 1$. The amount of re-welding would depend on the pressure; a typical efficiency might be $\eta = 1/2$. On reversed sliding, the new material would be passing partially re-welded material, and the efficiency would drop further, say to 1/4. (Even on the initial deformation, the material nearest the new tip is passing an old crack face that has been rubbed for some distance and is likely to weld more easily. Thus the degree of coherence along the fresh crack is likely to vary, as indicated in Figure 7a).

Now consider a dislocation running off to the side, tending to produce crack opening, as shown in Figure 7b. There is no re-welding, and the crack growth efficiency relative to the average flank coordinate is $\eta = 1$. A dislocation of the same sign, moving downwards and to the left along the

same cross-slip plane through the crack tip would give the same final configuration as that of Figure 7b. A dislocation of opposite sign, however, would bring the crack flanks together, as shown in Figure 7c. Because there would be relatively little pressure on the glide plane as it slid closed, the magnitude of the growth efficiency would still be approximately $|\eta| = 1$. It should be noted, however, that the crack growth would actually be negative during this half cycle ($\eta = -1$). This cancels out the growth shown in Figure 7b.

If a dislocation of sign opposite to that shown in Figure 7b were to travel upward to the right along the same slip plane it would require interference at the crack tip. Such flow would more likely arise from dislocations running in towards the tip from outside. Any that reach the tip are likely to travel along planes somewhat behind it, as shown in Figure 7d. The growth efficiency is $\eta = 1$ because there is no re-welding.

The above series of displacements has consisted of coplanar slip (i.e., slip on the crack plane) followed by cross-slip. Reversing the order, to cross-slip followed by coplanar slip, gives similar results except that producing crack opening first will increase the efficiency of crack growth due to slip on the crack plane.

Shear on Opposing Planes Through the Crack Tip

The combination of dislocations of opposite sign running out from the crack tip along the same plane, as shown in Figures 7b and 7c, amounts to homogeneous shear on the cross-slip plane in front of the crack. Various sequences of such cross-slip, combined with coplanar (crack-plane) slip, are shown in Figure 8. Figure 8a shows the same process as Figure 7a. Similarly, Figure 8b shows the combination of the processes in Figure 7b and 7c. Cross-slip of the opposite sign is shown in Figure 8c. In the processes of both Figures 8b and 8c, the efficiency would be very small because only the discontinuities and oxide film at the very crack tip would be spread out along the new cross-slip plane, tending to weaken it. For later reference, the effects of both signs of slip on the other cross-slip plane through the crack tip are shown in Figures 8d and 8e.

Now consider cross-slip *followed* by coplanar slip. Initial cross-slip leaves the patterns shown in Figures 8b-e, but with no fresh cracking on horizontal surfaces. The corresponding patterns after coplanar slip are shown as Figures 8f-i in the second column of Figure 8. The reversal of that for Figure 8b, shown in Figure 8f, gives the same crack advance but the spur crack has been left behind. Reversing the sequence of Figure 8c gives the same pattern as before, as shown in Figure 8g. Reversing the sequence of Figure 8d gives a new result, however. Crack plane slip of the opposite sign will tend to come in at the new crack tip and open up a hole, as shown in Figure 8h. The crack growth efficiency will also be higher on reversing the sequence. This lack of commutativity will be awkward to incorporate into an overall theory of crack growth. Finally, reversing the sequence of Figure 8e gives the same pattern as before, shown in Figure 8i.

This discussion indicates some of the features that would be required in a general criterion of fracture under combined compression and shear. Experiments so far (Jones and Chisholm [17]) deal with the coplanar slip deformation found to be most important here for these horizontal cracks in a rail, but have not included the transverse compression. Monotonic shear with pressure has been studied by Tipnis and Cook [18].

CONCLUSIONS

1) While the plasticity of a crack in a rail head is complicated, it can be approximated with reasonable economy.

2) For horizontal cracks in the elastic-plastic regime, the flow is primarily shear along the plane of the crack.

3) A change in crack direction would appear to require either a higher load or shear components of load.

4) A criterion for crack growth under sliding and compression is needed, and will have to take re-welding into account as a limiting case.

ACKNOWLEDGEMENT

The interest in and support of this work by the Transportation Systems Center, Department of Transportation, under contract TS-11653, is deeply appreciated. The help of Robert M. Russ with the computations, Erika M. L. Babcock with the typing, and Charles V. Mahlmann with the illustrations is also gratefully acknowledged.

REFERENCES

1. FEDERAL RAILROAD ADMINISTRATION, Office of Safety, Bulletin 141, Washington, D. C., 1972.
2. NATIONAL TRANSPORTATION SAFETY BOARD, Rept. RSS-74-1, Washington, D. C., 1974.
3. IRWIN, G. R., J. Applied Mech., 24, 1957, 361.
4. WILLIAMS, M. L., J. Applied Mech., 24, 1957, 109.
5. HUTCHINSON, J. W., J. Mech. Phys. Solids, 16, 1968, 13.
6. HUTCHINSON, J. W., J. Mech. Phys. Solids, 16, 1968, 337.
7. RICE, J. R. and ROSENGREN, G. F., J. Mech. Phys. Solids, 16, 1968, 1.
8. RICE, J. R., Fracture, 2, ed. H. Liebowitz, Academic Press, New York, 1968, 191.
9. McCLINTOCK, F. A., Fracture, 3, ed. H. Liebowitz, Academic Press, New York, 1971, 47.
10. JOHNSON, K. L., Proc. 4th U. S. Nat. Cong. Appl. Mech., Am. Soc. Mech. Eng., 2, 1962, 971.
11. RADZIMOVSKY, E. I., Univ. of Ill., Eng. Exp. Sta. Bull., 408, Urbana, 1953.
12. DUGDALE, D. S., J. Mech. Phys. Solids, 8, 1960, 100.
13. BARENBLATT, G. I., Advances in Appl. Mech., 1, eds. H. L. Dryden and T. von Karman, Academic Press, New York, N. Y., 1962.
14. CROOK, A. W., Proc. Inst. Mech. Eng., London, 171, 1957, 187.
15. PUSTEJOVSKY, M. A., Ph. D. thesis M. I. T., Cambridge, Massachusetts, 1976.
16. NEIMARK, J. E., J. Applied Mech., 35, 1968, 111.
17. JONES, D. L. and CHISHOLM, D. B., Fractography - Microscopic Cracking Processes, ASTM STP 600, eds. C. D. Brachem and W. R. Warke, 1976, 235.
18. TIPNIS, V. A. and COOK, N. H., J. Basic Eng., Trans. Am. Soc. Mech. Eng., 89D, 1967, 533.

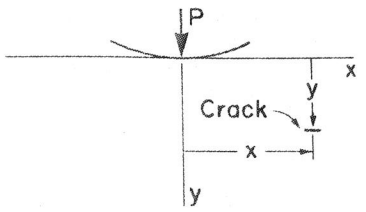

Figure 1 - Coordinates of crack relative to contact point

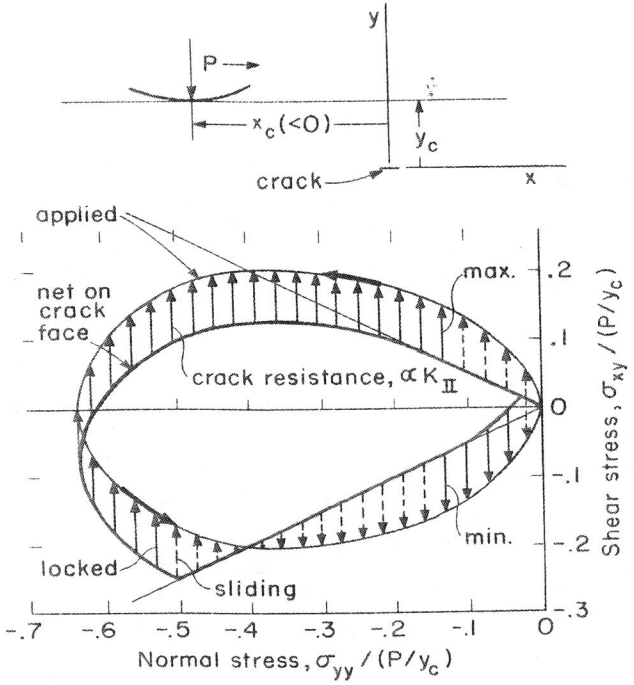

Figure 2 - Applied and crack face stresses on a buried crack

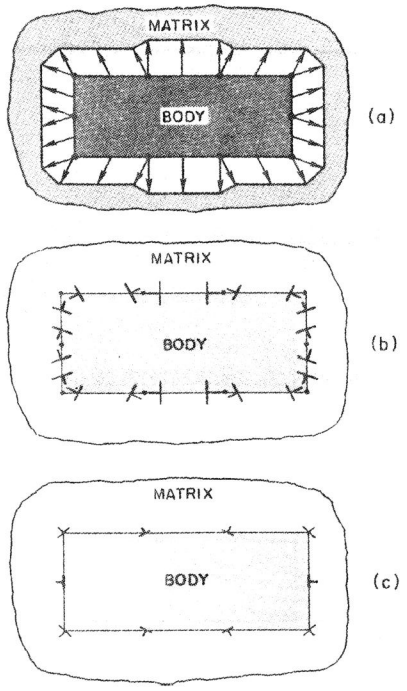

Figure 3 - Modelling biaxial tension on a body with translational displacement discontinuities or darts (a), giving dislocation dipoles on each segment (b), and resultant dislocations at nodes (c).

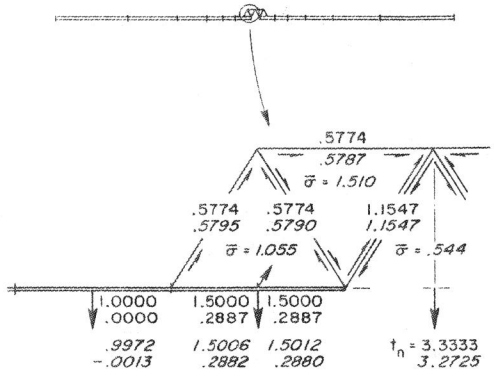

Figure 4 - Analytical and *computed* displacements and stresses for fully plastic test

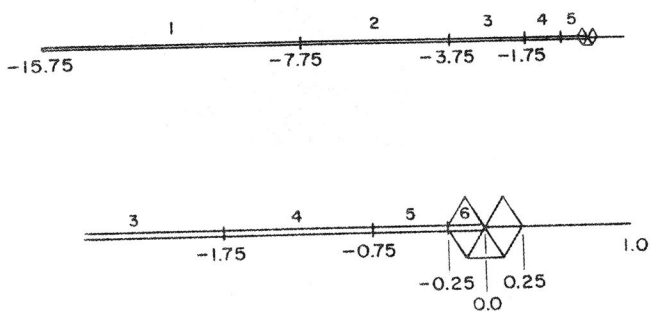

Figure 5 - Segments for modelling a crack with localized plastic flow

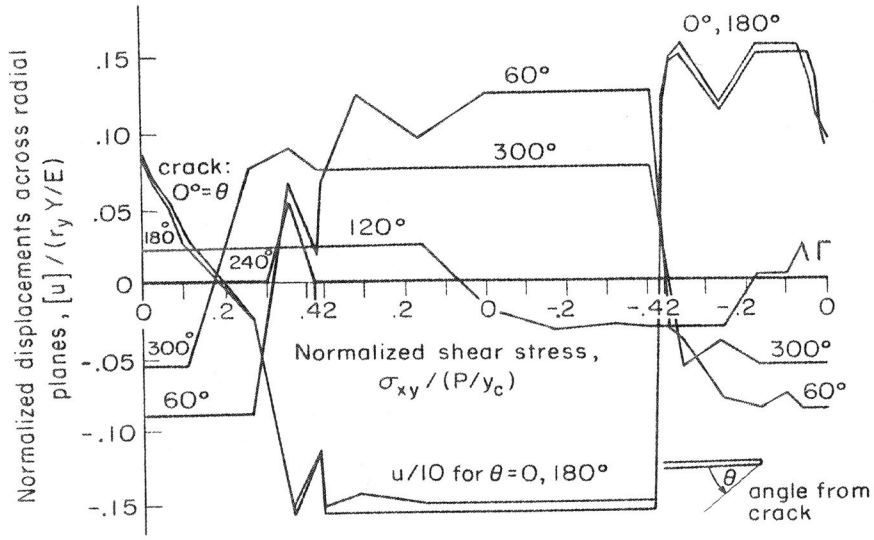

Figure 6 - Normalized displacement history across planes radiating from a crack tip under shear and pressure.

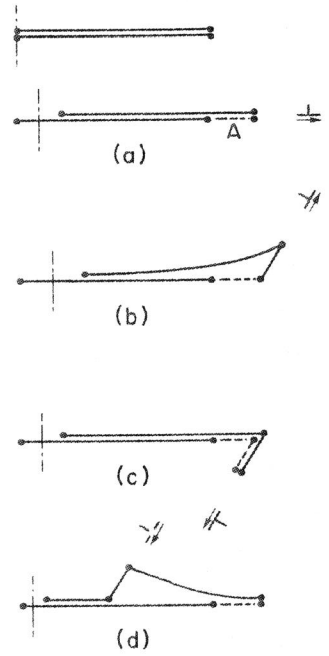

Figure 7 - Crack growth from slip on one radial plane at a time

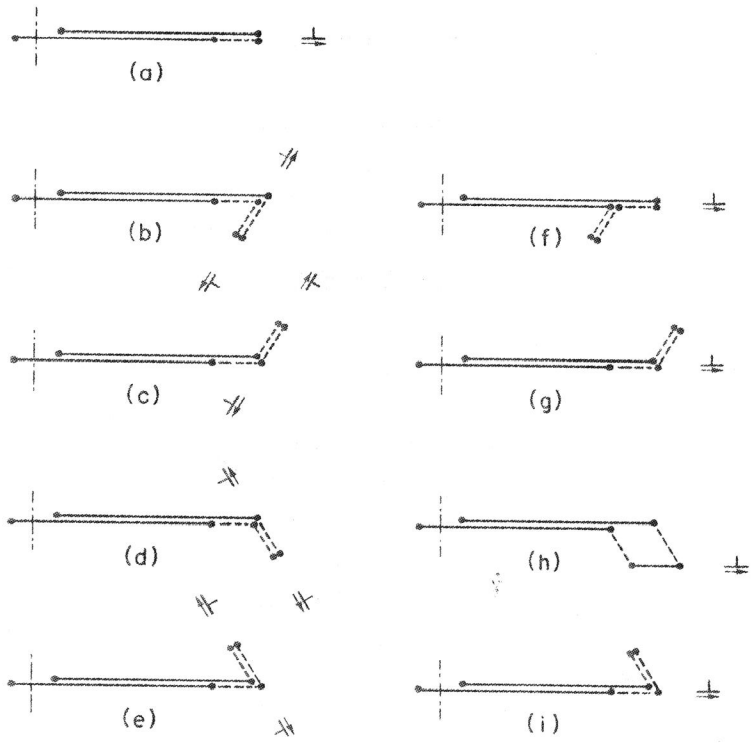

Figure 8 - Crack growth from co-planar slip (a) followed by cross-slip (b-e) and cross-slip followed by co-planar slip (f-i).